Plant, Cell & Environment

Plant, Cell and Environment (2015) **38**, 2462–2474 doi: 10.1111/pce.12562

Original Article

Improved method for measuring the apparent CO_2 photocompensation point resolves the impact of multiple internal conductances to CO_2 to net gas exchange

Berkley J. Walker[1,2] & Donald R. Ort[1,2,3]

[1]*Global Change and Photosynthesis Research Unit, USDA/ARS, Urbana, IL 61801, USA,* [2]*Institute of Genomic Biology and* [3]*Department of Plant Biology, University of Illinois, Urbana, IL 61801, USA*

ABSTRACT

There is a growing interest in accurate and comparable measurements of the CO_2 photocompensation point (Γ^*), a vital parameter to model leaf photosynthesis. The Γ^* is measured as the common intersection of several CO_2 response curves, but this method may incorrectly estimate Γ^* by using linear fits to extrapolate curvilinear responses and single conductances to convert intercellular photocompensation points (C_i^*) to chloroplastic Γ^*. To determine the magnitude and minimize the impact of these artefacts on Γ^* determinations, we used a combination of meta-analysis, modelling and original measurements to develop a framework to accurately determine C_i^*. Our modelling indicated that the impact of using linear fits could be minimized based on the measurement CO_2 range. We also propose a novel method of analysing common intersection measurements using slope–intercept regression. Our modelling indicated that slope–intercept regression is a robust analytical tool that can help determine if a measurement is biased because of multiple internal conductances to CO_2. Application of slope–intercept regression to *Nicotiana tabacum* and *Glycine max* revealed that multiple conductances likely have little impact to C_i^* measurements in these species. These findings present a robust and easy to apply protocol to help resolve key questions concerning CO_2 conductance through leaves.

Key-words: photosynthesis; photorespiration.

INTRODUCTION

Biochemical models of leaf photosynthesis are an invaluable tool to both predict plant response to climate change and identify potential targets to improve the efficiency of CO_2 fixation (Sage & Kubien 2007; Zhu *et al.* 2008). These models are also used to estimate terrestrial CO_2 exchange at the canopy and earth system scale (Drewry *et al.* 2010; Rogers *et al.* 2014). Models of net gas exchange combine the physiology of CO_2 fixation with CO_2 release from mitochondrial respiration and loss following the oxygenation of ribulose 1·5-bisphosphate carboxylase/oxygenase (Rubisco) by photorespiration. Leaf photosynthesis models are parameterized using the substrate gas (CO_2 and O_2) partial pressures, reaction kinetics of Rubisco, stoichiometry of CO_2 release per Rubisco oxygenation (α), and rates of daytime mitochondrial respiration (R_d; von Caemmerer & Farquhar 1981; von Caemmerer 2000). The CO_2 photocompensation point (Γ^*), the chloroplastic CO_2 partial pressure at which rates of Rubisco carboxylation equal rates of CO_2 loss from photorespiration, is a key parameter in these models and combines Rubisco specificity ($S_{c/o}$), O_2 partial pressure (O) and α according to

$$\Gamma^* = \frac{\alpha O}{S_{c/o}} \quad (1)$$

Γ^* can be estimated from the common intersection of photosynthetic chloroplastic CO_2 response (A-C_c) curves measured under sub-saturating irradiances (Fig. 1; Laisk 1977; Brooks & Farquhar 1985). The common intersection is predicted to relate to Γ^* assuming either RuBP-regeneration-limited or Rubisco-limited photosynthesis and has the added benefit of providing an estimate of R_d at the y-value of the common intersection (Laisk 1977; von Caemmerer *et al.* 1994). Since this intersection is determined from chloroplastic CO_2 partial pressures, CO_2 conductance from the intercellular air space to the chloroplast must be known to obtain a true estimate of Γ^* since in practice, the photosynthetic response to intercellular CO_2 concentrations (A-C_i) is measured (von Caemmerer *et al.* 1994). CO_2 conductance into the chloroplast has traditionally been considered as a single mesophyll conductance (g_m) and relates Γ^* to C_i^* according to

$$\Gamma^* = C_i^* + R_d/g_m \quad (2)$$

where C_i^* is the CO_2 partial pressure at the intersection. Γ^*, and by extension C_i^*, has a temperature dependency, usually considered dependent on the temperature response of Rubisco specificity. Currently the measured temperature response of Γ^* or C_i^* determined from plants grown at a common temperature is used to model the temperature response of photosynthesis in climate change models (Bernacchi *et al.* 2001, 2002; Walker & Cousins 2013; Walker *et al.* 2013).

Correspondence: D. R. Ort. e-mail: d-ort@illinois.edu

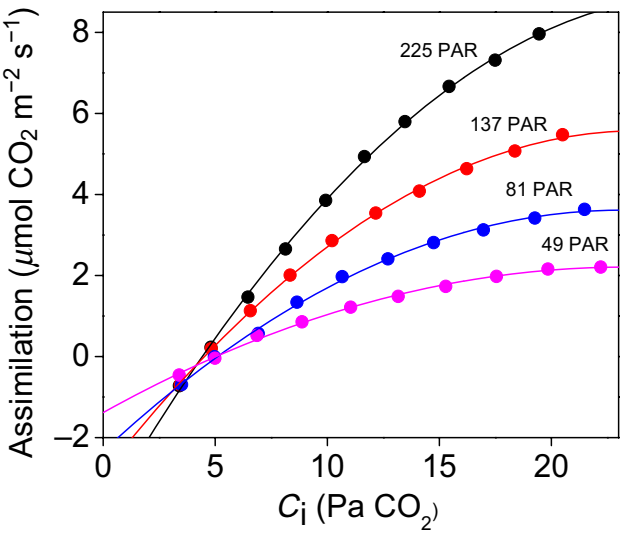

Figure 1. An example intercellular CO_2 photocompensation point (C_i*) measurement using the common intersection method. Shown is a single replicate of a measurement of the *N. tabacum* CO_2 response of net CO_2 assimilation measured at four sub-saturating light intensities indicated by the PAR values on the plot with lines representing a trinomial fitting function.

Recently, it has been questioned if a single diffusive term is adequate to describe mesophyll conductance. Several variations of a multiple diffusion model account for CO_2 movement through the cell wall and chloroplast separately and allow CO_2 produced from photorespiration in the mitochondria to pass directly to the intercellular space (Tholen & Zhu 2011; Tholen *et al.* 2012; Busch *et al.* 2013; von Caemmerer 2013). These models predict that multiple conductances to CO_2 would increase actual C_i* and not produce a common intersection, but it is unclear how much they impact current estimations of C_i*.

It has also been questioned if C_i* intersections from linear fits can properly be used in common intersection measurements since the CO_2 response of photosynthesis is curvilinear (Gu & Sun 2014) Linear fits are modelled to underestimate C_i* and R_d over a given CO_2 range. Since the initial portions of A-C_i curves are closer to linear than portions under higher CO_2 (Fig. 1), linear fits are expected to introduce more error when applied over a broad range of CO_2 values, and less error if applied to a narrow range. The impact of specific CO_2 ranges on final C_i* values has not yet been shown.

These uncertainties highlight potential issues in using the common intersection method to determine both C_i* and R_d that would compromise current parameterization of biochemical models of leaf photosynthesis and impact modelled CO_2 exchange. In addition to impacting physiological measurements, multiple diffusion paths could also decrease the efficiency of photorespiration if the resistance to CO_2 diffusion was very large through the chloroplast relative to the cell wall. Such a difference in resistances would allow photorespired CO_2 to diffuse from the mitochondria into the intercellular airspace and escape the leaf through the stomata (Tholen & Zhu 2011; Tholen *et al.* 2012; Busch *et al.* 2013; von Caemmerer 2013). These potential issues with traditional common intersection determination of C_i* and R_d suggest that a more sensitive and robust protocol is needed to account for the impact of CO_2 measuring range and the possible significance of multiple conductance pathways and thus conductance values.

To determine the impact of linear fitting and different assumptions of CO_2 conductance to common intersection measurements of C_i*, we analysed various reports of C_i* published over the last 40 years. In addition to this meta-analysis, we performed additional measurements and modeling of common intersection curves to quantify how estimates of C_i* might be biased and determine measurement conditions that limit this bias. We introduce a new method for interpreting common intercept data (slope–intercept regression) that should produce more accurate determinations of C_i* and R_d and can determine if multiple conductances to CO_2 are significant (see Theory below).

THEORY

The common intersection method determines C_i* by averaging the intersection of several A-C_i curves measured under several sub-saturating irradiances (Fig. 1). In practice, these lines seldom converge on a single point and it is common to remove intersection values or to re-measure until all intersections are within two standard deviations (or some other metric) from the mean (e.g. Weise *et al.* 2015). Determining a common intersection is complicated by the fact that the intersection of two lines is more sensitive to experimental noise when slopes are similar, since small differences in slope can produce large differences in intersections between in lines that are approaching parallel. Conversely, the intersection of two lines with very different slopes is more resilient to experimental noise. An important shortcoming of the common intersection method is that all intersections are equally weighted ignoring the fact that some of the intersections are more robust than others. This problem becomes increasingly apparent as more than three irradiances are used to determine C_i* and when the slopes of neighboring lines become more similar.

We propose a variation on the common intercept method that we term the slope–intercept regression as a way to appropriately analyse common intercept data while giving more weight to intersections that are more robust. The value of x at the intersection (C_i*) of the linear portion of two A-C_i curves can be calculated from their slopes (m_1 and m_2) and y-intercepts (b_1 and b_2) as

$$C_i^* = \frac{b_1 - b_2}{m_2 - m_1} \tag{3}$$

and the value of y at the intersection (R_d) as

$$R_d = mC_i^* + b \tag{4}$$

Traditionally the C_i* and R_d values for each combinations of line intersections is calculated graphically or with these equations and averaged together, with each line pairing given equal weight.

The slope–intercept regression analysis begins by plotting the m values on the x-axis and the b values on the y-axis from each individual A-C_i curve. A linear regression is made of this plot producing a standard linear equation except that the x and y values represent the m and b from individual CO_2 response measurements. The slope of this regression (m_{reg}) is therefore

$$m_{reg} = \frac{b_2 - b_1}{m_2 - m_1} \quad (5)$$

which, when multiplied by –1 and rearranged, is equal to C_i* (Eqn 3). The y-intercept of this line also represents R_d, as can be seen when the slope–intercept regression line is expressed using negative C_i* for slope (Eqn 5) and the y-intercept of the regression (b_{reg}) as

$$b = -C_i^* m + b_{reg} \quad (6)$$

that when combined with Eqn 4 produces

$$R_d = b_{reg} \quad (7)$$

This method will have an advantage over simply averaging intercepts from each combination of A-C_i curves since the regression weights values of m that are further apart more strongly in its determination of C_i* than those that are close together. It should be noted that a variation of the slope-intercept regression technique is often used in computer-assisted image processing and can be applied to more complicated curves within images (Duda and Hart, 1972).

This method could also help determine if multiple conductances to CO_2 across the cell wall and chloroplast impact measurements of C_i* using the common intersection method. The slope–intercept regression of individual A-C_i curves would not be linear assuming multiple CO_2 conductances between the cell wall and chloroplast since C_i* (the slope of this relationship) is predicted to increase when rates of photosynthesis and photorespiration are high (Tholen & Zhu 2011; Tholen *et al*. 2012; Busch *et al*. 2013; von Caemmerer 2013). This condition would produce a curvilinear instead of linear relationship, with the degree of curvature increasing as more photorespired CO_2 is lost from the mitochondria into the intercellular airspace when the ratio of chloroplastic to cell wall increases.

We used a brute-force modelling approach to determine the impact of multiple internal conductances to the relationship between the slope and intercept of the initial portions of A-C_i curves measured under sub-saturating irradiances. To determine slope and intercept values, we assumed six CO_2 partial pressures in the mesophyll (C_m, 25, 35, 45, 65 and 75 Pa CO_2) and solved for C_c using a quadratic solution of a RuBP regeneration-limited model accounting for multiple conductances, expressed here as resistances (equation A29 in von Caemmerer 2013)

$$C_c = \frac{\left(C_m - \frac{r_c J}{4} - 2\Gamma^*\right) + \sqrt{\left(C_m - \frac{r_c J}{4} - 2\Gamma^*\right)^2 + 4(C_m 2\Gamma^*)}}{2} \quad (8)$$

where r_c represents the chloroplastic resistance to CO_2 transfer and J represents the rate of electron transfer. Net CO_2 assimilation (A) was then determined assuming RuBP regeneration-limitation and cell wall resistance to CO_2 transfer (r_w) according to

$$A = (C_i - C_m)/r_w \quad (9)$$

To determine how slope–intercept regression is impacted by different resistances to CO_2 transfer, we assumed four different scenarios ($r_c = 0$ and $r_w = 0.3$; $r_c = 0.06$ and $r_w = 0.24$; $r_c = 0.15$ and $r_w = 0.15$; $r_c = 0.3$ and $r_w = 0$ m^{2s} Pa mol^{-1}). Different slopes and intercepts were generated by varying J and the model used the R_d value from the slope–intercept regression (Eqn 7) and a Γ* value that gave a best fit with the lowest measured irradiance slope and intercept.

This paper uses measured and modelled data to evaluate slope–intercept analysis and demonstrates that is a superior way to interpret common intercept data using both measured and modelled datasets. We also use slope–intercept analysis to explore if multiple intercellular conductances to CO_2 significantly impact measurements of C_i* in *Nicotiana tabacum* and *Glycine max*.

MATERIAL AND METHODS

Literature reports of common intercept values

Reported values of C_i* and Γ* were gathered from an extensive literature search using standard search tools (SCOPUS, Web of Science and Google Scholar) for 'CO_2 compensation point', 'Day respiration' and 'Laisk method'. We additionally searched individual journal archives and papers referencing papers likely to contain reported values. If necessary, C_i* and Γ* values were converted to the SI units of Pa from μmol or μbar CO_2 using the elevation of the measurement location to determine atmospheric pressure. Γ* values were converted to C_i* using reported values of g_m and R_d (Eqn 2) and temperature corrected to 25 °C using a derivation of the temperature response of *N. tabacum* (Bernacchi *et al*. 2001). The CO_2 range used in the measurement, species, and species functional type was recorded for statistical analysis. Species names listed are as categorized by the United States Department of Agriculture Natural Resources Conservation Service PLANTS Database using the Cronquist taxonomic system for flowering plants using the information available from the primary publication (Cronquist 1981; USDA 2015). A full list of non-abbreviated species names used is presented as Supporting Information Table S2.

Growth conditions

N. tabacum were sown in covered germination flats containing potting soil (Sunshine Mix #1 LC1, SunGro Horticulture, Agawam, MA, USA). After 2–3 weeks, plants were transplanted to 2 L pots and further grown for an additional 2–3 weeks (4–6 weeks total) until large enough for gas exchange. *G. max* were sown in 3 L pots with a top dressing

of Osmocote (Scotts Miracle-Gro, Marysville, OH, USA). Both *N. tabacum* and *G. max* plants were grown in a climate-controlled cabinet (Conviron, Winnipeg, Manitoba, Canada) with day/night cycles of 11/13 h and 25/23 °C under an irradiance of 300 μmol m^{-2} s^{-1}. Plants were watered as needed and fertilized weekly (Peters 20-20-20, J.R. Peters, Allentown, PA, USA).

Measurements of C_i*

The youngest fully expanded leaves of 30–40-day-old plants were used for gas exchange for *N. tabacum* and *G. max*. Gas exchange was performed using a Li-Cor 6400 XT modified to reach low CO_2 partial pressures using a 6 cm^2 chamber with a red/blue light source (Li-Cor Biosciences, Lincoln, NE, USA; Li-Cor Biosciences 2010). To determine irradiances that would result in an even distribution of photosynthetic rates for C_i* determinations, the photosynthetic light response of each species was first measured at 20 Pa CO_2. *N. tabacum* was measured under irradiances of 225, 137, 80 and 49 μmol m^{-2} s^{-1} and *G. max* under 300, 175, 120, 80 and 50 μmol m^{-2} s^{-1}. For each light intensity, assimilation was measured at five intercellular CO_2 partial pressures ranging from 3.5 to 9.5 Pa CO_2.

Accounting for CO_2 leakage during gas exchange measurements is essential for determining accurate assimilation rates when measurement CO_2 is below atmospheric partial pressures (Long and Bernacchi, 2003; Flexas *et al*. 2007). Assimilation measurements were corrected for CO_2 leakage between the chamber and surrounding atmosphere according to the manufacturer's instruction. To validate this correction method, leaves were measured in the dark under identical CO_2 measuring regimes as used during the common intersection measurements. The photosynthetic rate in the dark (dark respiration) should not be sensitive to changes in CO_2, so measured differences were attributed to gasket leakage. This gasket leakage for each CO_2 partial pressure was then used to correct common intersection measurements. Both methods of leak correction produced similar values of C_i* and R_d. Values corrected according to the manufacturer's instruction were presented.

Prior to C_i* determinations using the common intersection method, plants were acclimated at 39 Pa CO_2 until photosynthesis reached steady state to activate Rubisco. After each change in irradiance, a measurement was made at 39 Pa CO_2 to maintain Rubisco activation. The C_i* and R_d values were determined both from the average *x*- and *y*-intersection values (common intersection) and the regression of the slopes and *y*-intercepts from each irradiance (slope–intercept regression, see Theory).

Sensitivity analysis of C_i* and R_d to CO_2 measuring range

The impact of using linear fits to calculate common intersection values of C_i* and R_d was determined using standard biochemical models of Rubisco- and RuBP-regeneration-limited photosynthesis (von Caemmerer & Farquhar 1981; von Caemmerer 2000). C_i* and R_d were defined as the averaged intersection of three A-C_i curves modelled assuming Rubisco limitation at the highest irradiance and RuBP-regeneration at the lower irradiances. Constant values of K_c, K_o, Γ* and R_d (25.9 Pa, 17.9 kPa, 3.86 Pa and 1 μmol m^{-2} s^{-1}) were used with a V_{cmax} at the highest irradiance of 68.5 μmol m^{-2} s^{-1}. We selected values of rates of electron transport for the lower two light intensities to give an even distribution of slopes among each modelled irradiance for each CO_2 measuring range since a researcher would select light intensities that produce an even spread of slopes. These J values ranged between 67 and 21 μmol e^- m^{-2} s^{-1}. The model was solved for six evenly spaced chloroplastic CO_2 partial pressures (C_c) for each CO_2 range. The CO_2 range started at 35 Pa CO_2 and ended at an uppermost value that started at 50 and increased to 235 Pa CO_2 by increments of 10–40 Pa CO_2. These C_c partial pressures were converted to C_i partial pressures assuming a single linear pathway g_m value of 3.33 mol m^{-2} s^{-1} MPa^{-1}. The partial A-C_i curves were then fitted using a linear model and C_i* and R_d determined as the averaged value for each combination of intersections of the three lines.

Simulations of common intercept measurements

To compare the accuracy of different methods of determining C_i* and R_d values from common intersection data, we simulated a number of initial slopes of A-C_i curves assuming different numbers of light intensities. The simulation began by first generating an ideal common intersection measurement consisting of lines that intersected at the parameterized C_i* and R_d values with evenly spaced slopes. To represent experimental data, we then selected a random slope from a normal distribution with a mean equal to our ideal values and a standard deviation based on the measured variation in *N. tabacum*. The simulation used the experimental relationship between slope and standard deviation to parameterize the variance since our experimental data indicated that the standard deviation varied with slope. These simulated experimental data were determined for each line to produce a single replicate of simulated experimental data. The C_i* and R_d for each of these replicates was then determined in one of three ways: (1) as the average of all combinations of intersections, (2) as the average of all combinations of intersections following outlier removal defined as intercept values more or less than two standard deviations from the original average or (3) using slope–intercept regression. This simulation was performed 1 000 000 times using 2–8 separate lines with evenly spaced slopes to represent the impact of using additional light intensities. Modelling was performed using R (R Core Team 2013) and is available as Supporting Information Table S2.

Impact of low CO_2 to photosynthesis

We performed additional gas exchange to determine the impact of low CO_2 partial pressures to Rubisco activation

and optimize measuring regimes. Gas exchange was performed using the Li-Cor 6400 XT on fully expanded leaves of 30–40-day-old *N. tabacum* by first acclimating leaves at 40 Pa CO_2 and an irradiance of 390 μmol m^{-2} s^{-1} until they reached steady-state assimilation and conductance values. Following acclimation, the CO_2 partial pressure was changed to either 1, 6, 8, 10 or 120 Pa CO_2 for 7 min, then returned to 40 Pa CO_2 for 20 min. This cycle was repeated on the same leaf with increasing periods of time at the lowered CO_2 (12, 17 and 22 min). Data were recorded every minute and the infrared gas analysers were matched following each CO_2 transition. Presented values were normalized by dividing the measured assimilation rate by the assimilation rate immediately before transition to lower CO_2.

Statistics

A one-way ANOVA for measurement temperature, CO_2 measuring range and species type was used to test significance ($P < 0.05$) of interactions within compiled C_i* values. One-way ANOVA was also performed to determine significant differences between measurements of C_i* and R_d. All ANOVA were followed with a Tukey's post-hoc test and determined using statistical software (OriginPro 9.0, OriginLab, Northhampton, MA, USA).

RESULTS

Literature C_i* values varied significantly with measurement temperature

To determine the variation in literature values of C_i*, we compared values from 34 published and unpublished sources (Fig. 2 and Supporting Information Table S1). The temperature response of C_i* measured in *N. tabacum* was more pronounced than raw C_i* values reported in the literature (Fig. 2a). C_i* normalized to 25 °C using the temperature response of *N. tabacum* ranged from an average of 3.49 Pa CO_2 in *Oryza* species to 5.57 Pa CO_2 in *Acer rubrum*. Interestingly, the only significant correlation in values of C_i* was with measurement temperature despite all values being normalized to using the temperature response of *N. tabacum* (Fig. 2b). Temperature-normalized C_i* values measured at lower temperatures (20 °C or lower) were significantly higher than measurements made at 25 °C. This trend continued with C_i* values measured at higher temperatures (30 °C or higher). There were no significant correlations between literature C_i* and the CO_2 range used in the measurement or species type (data not shown).

Modelled impact of uppermost CO_2 range on common intersection measurements

We next modelled the impact of CO_2 measuring range on common intersection determination of C_i* and R_d assuming a single linear mesophyll conductance pathway (Fig. 3). Both C_i* and R_d were close to the values used to parameterize the

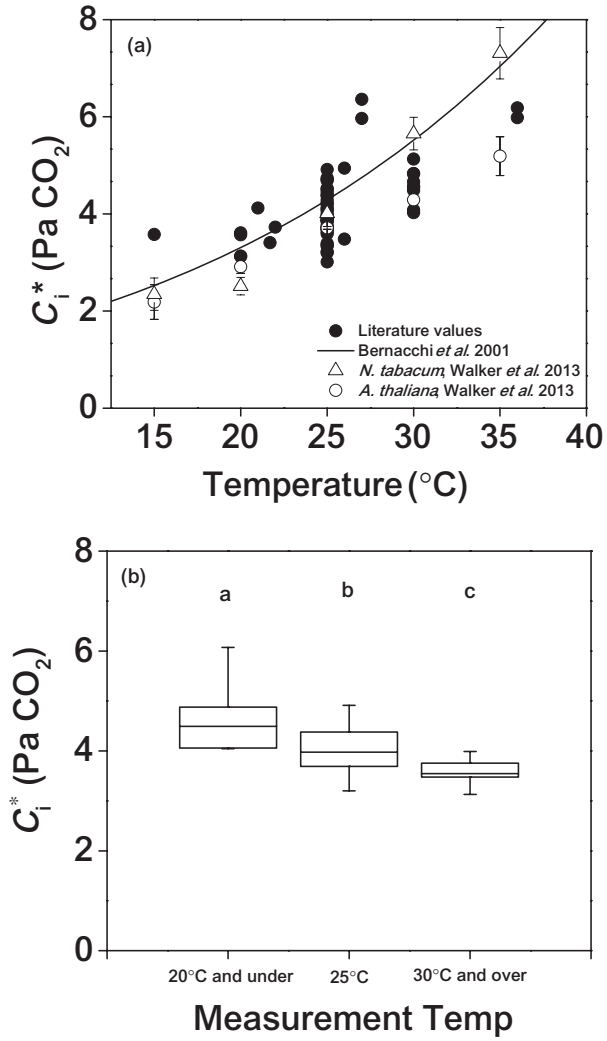

Figure 2. The intercellular CO_2 photocompensation point (C_i*) as reported in the literature according to measurement temperature (a) and a categorical boxplot (b). The temperature response (a) shows absolute literature values with both the temperature response of Bernacchi *et al.* 2001 (solid line) and temperature response of *N. tabacum* and *A. thaliana* from Walker *et al.* 2013. The boxplot values (b) were normalized from measurement temperature to 25°C using the temperature response reported in Bernacchi *et al.* 2001. Boxes depict a 75% confidence interval with whiskers indicating the 95% interval. Significant ($p < 0.05$) interaction of C_i* with measuring range according to ANOVA analysis is indicated by different letters above each plot. Data was obtained from a variety of reports (Laisk, 1977; Kirschbaum and Farquhar, 1984; Brooks and Farquhar, 1985; Jacob and Lawlor, 1993; Berry *et al.*, 1994; Villar *et al.*, 1994; von Caemmerer *et al.*, 1994; Balaguer *et al.*, 1996; Häusler *et al.*, 1996; Bunce, 1998; Evans and Loreto, 2000; Bernacchi *et al.*, 2001; Peisker and Apel, 2001; Igamberdiev *et al.*, 2004; Pons and Westbeek, 2004; Guo *et al.*, 2005; Galmés *et al.*, 2006; Schneidereit *et al.*, 2006; Warren and Dreyer, 2006; Flexas *et al.*, 2007; Kebeish *et al.*, 2007; Weston *et al.*, 2007; Li *et al.*, 2009; Tomaz *et al.*, 2010; Cano *et al.*, 2011; Cousins *et al.*, 2011; Tholen and Zhu, 2011; Douthe *et al.*, 2012; Gilbert *et al.*, 2012; Tholen *et al.*, 2012; Busch *et al.*, 2013; Giuliani *et al.*, 2013; Sage *et al.*, 2013; Walker *et al.*, 2013; Walker and Cousins, 2013; Walker *et al.*, 2014; Weise *et al.*, 2015).

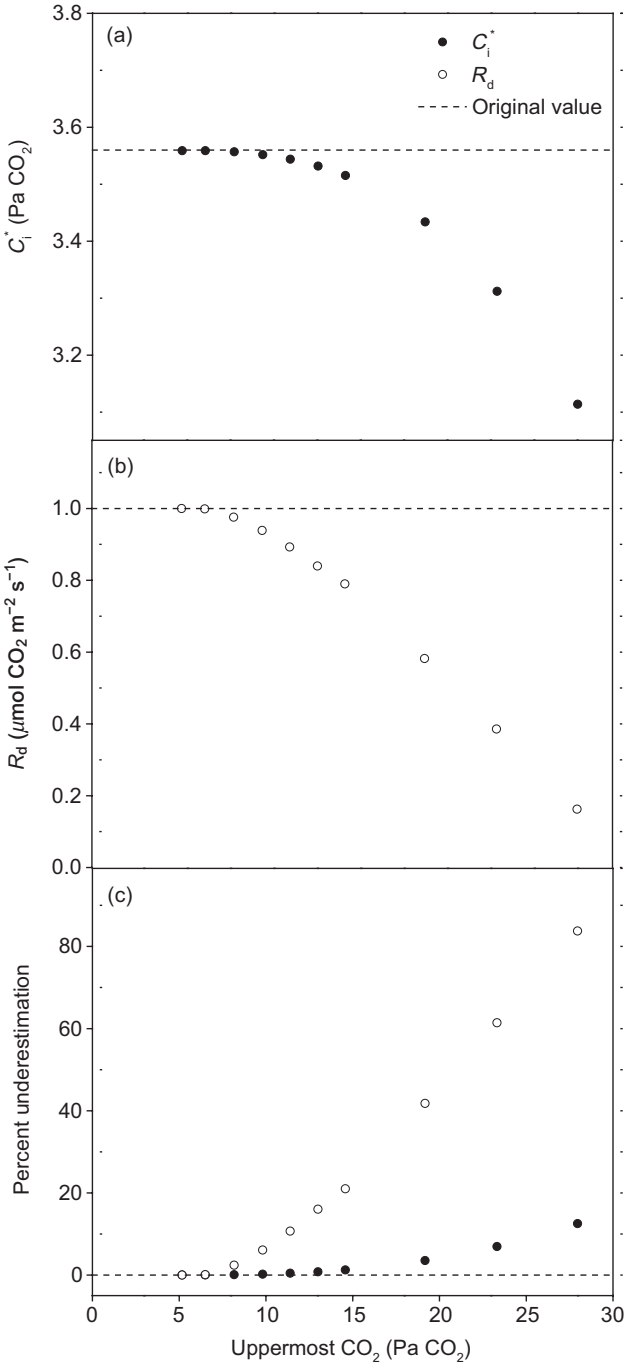

Figure 3. Impact of uppermost CO_2 partial pressure on estimates of C_i* (a) and R_d (b) using the common intersection method. Values of C_i* (a) and R_d used in the modelled parameterization are shown with dotted lines. Common intersection measurements were modelled assuming three light intensities as outlined in the Materials and Methods. Also shown are the percent underestimations under increasing uppermost CO_2 partial pressures (c).

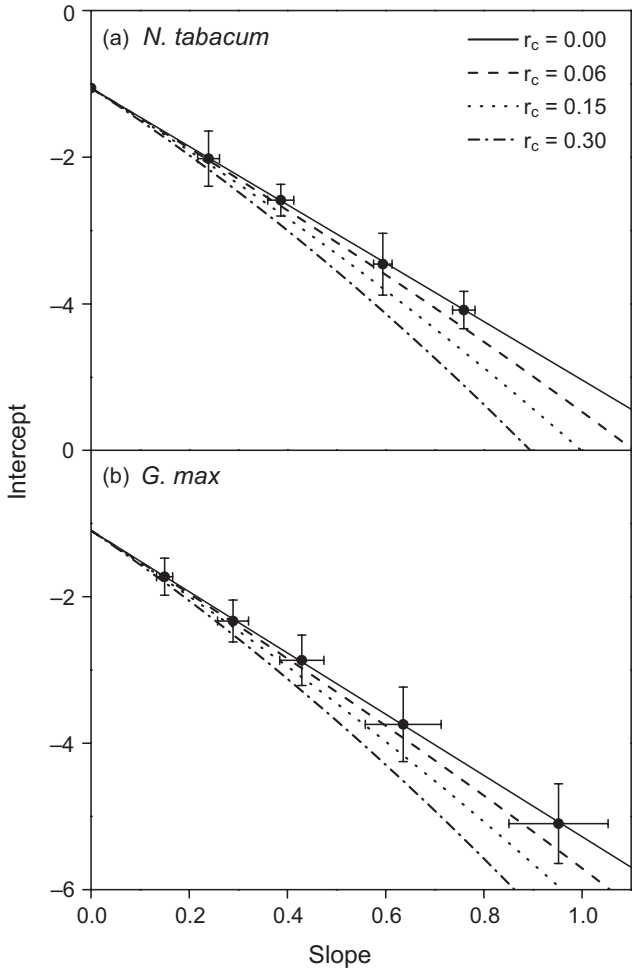

Figure 4. Slope–intercept regression analysis of common intercept measurements in *N. tabacu*m (a) and *G. max* (b). Slope and intercept measurements from the initial slope of photosynthetic CO_2 response were determined under 4–5 sub-saturating irradiances. Lines represent the modelled relationship between slope and intercept assuming multiple internal resistances to CO_2 and increasing chloroplastic CO_2 resistance (r_c). Means of n = 4–5 ± SD are shown. The model assumed Γ* and R_d were 4.11 Pa and 1.1 m^2 s^{-1} for *N. tabacum* and 4.31 Pa and 1.1 μmol m^{-2} s^{-1} for *G. max*. Slopes and intercepts were determined using a linear fit of six mesophyll CO_2 partial pressures between 2.5 and 7.5 Pa and total (See Theory).

model when the uppermost CO_2 value was low, but decreased as the uppermost value of CO_2 increased (Fig. 3a,b). When uppermost values of CO_2 were below 10 Pa CO_2, C_i* was underestimated by less than 1% and R_d by less than 10% (Fig. 3c). These percent underestimations did not change significantly when models were repeated with R_d and g_m values either half or double that assumed in the presented data (data not shown).

Slope–intercept regression in *N. tabacum* and *G. max*

The relationship between the slope and intercept of common intercept measurements in both *N. tabacum* and *G. max* were strongly linear (Fig. 4). The average coefficient of determination (R^2) for a linear model was 0.997 ± 0.001 and 0.999 ± 0.000 for *N. tabacum* and *G. max*. These linear models

	N. tabacum		*G. max*	
	C_i* (Pa CO_2)	R_d (μmol m^2 s^{-1})	C_i* (Pa CO_2)	R_d (μmol m^2 s^{-1})
Common intersection	3.94 ± 0.04	1.07 ± 0.35	4.06 ± 0.23	1.03 ± 0.21
Slope-int. reg.	4.00 ± 0.07	1.04 ± 0.33	4.08 ± 0.24	1.02 ± 0.22

Table 1. Comparison of C_i* and R_d determined from CO_2 assimilation curves measured under sub-saturating illumination using two different methods

CO_2 gas exchange in *N. tabacum* and *G. max* were measured under 4–5 sub-saturating light intensities and intercellular CO_2 partial pressures ranging from 3.5–9.5 Pa CO_2. C_i* and R_d were determined as the averaged x and y value for the intersections of each light intensity (common intersection) or from the regression of the slope and intercept of all the light intensities together (slope-int. reg.). Means of $n = 4–5 \pm$ SD are shown. There were no significant differences between method of determining C_i* or R_d within species according to ANOVA analysis and Tukey post-hoc test.

produced C_i* and R_d values similar to those determined using the averaged intersection of each A-C_i curve (Table 1). The modelled relationship between the slope and the y-intercept became increasingly non-linear as the ratio of r_c to r_w increased.

We additionally used the modelled relationship between the slope and intercept of A-C_i curves in response to r_c to r_w in *G. max* to determine how different resistances would impact apparent C_i* and R_d measurements using slope–intercept regression (Table 2). We found that increasing the ratio of r_c to r_w increased apparent C_i* values by up to 45% and decreased R_d by up to 30%.

Modelled simulation of common intercept interpretation using three different analysis techniques

The impact of determining C_i* and R_d from common intersection measurements was simulated using the measured variation of *N. tabacum* A-C_i measurements and number of light intensities between two and eight (Fig. 5). When two light intensities were used, all methods of determining C_i* and R_d produced the same values and variation. When three or more light intensities were used, values of C_i* and R_d varied little with additional measuring light intensities and approached the modelled input when determined using averaged intercepts following outlier removal or the slope–intercept method. When all the intercepts were averaged with no outlier removal, C_i* and R_d showed high variation, regardless of light intensities used or even after simulating 1 000 000 common intersection measurements. The simulated variation of C_i* and R_d determined using averaged intersections following outlier removal or the slope–intercept method decreased with increasing number of light intensities, but additional light intensities above five had only marginal improvement in decreasing variation. The slope–intercept regression produced the least variation at every light intensity above two out of all the methods to determine C_i* and R_d and involved no outlier removal.

Impact of measurement CO_2 on net photosynthesis

We next determined how net photosynthetic CO_2 assimilation is impacted during long periods of leaf exposure to low CO_2. This control is important since it is possible for a leaf to remain for long periods at very low CO_2 depending on measuring regime during a common intercept measurement. Net CO_2 assimilation at 40 Pa CO_2 showed no decrease after exposure to 8 Pa CO_2 or greater for up to 22 min (Fig. 6a). Following 7 min exposure to 1 or 6 Pa CO_2 there was similarly no impact to net CO_2 assimilation at 40 Pa CO_2 (Fig. 6). Following a 12 min exposure to 1 or 6 Pa CO_2, there was a transient decrease in net CO_2 assimilation that returned to starting values after around 5 min. Net CO_2 assimilation took much longer to recover following a 17 min exposure to 1 or 6 Pa CO_2 and took the most time following a 22 min exposure.

	$r_c = 0$, $r_w = 0.3$	$r_c = 0.06$, $r_w = 0.24$	$r_c = 0.15$, $r_w = 0.15$	$r_c = 0.3$, $r_w = 0$
C_i* Pa CO_2	4.19 (0%)	4.67 (11%)	5.26 (25%)	6.07 (45%)
R_d μmol m^{-2} s^{-1}	1.1 (0%)	1.0 (9%)	0.9 (19%)	0.8 (30%)

Table 2. Impact of multiple conductances on apparent C_i* and R_d measured using slope–intercept regression

A slope–intercept regression was made on five modelled electron transport rates (9, 16, 24, 36 and 55 μmol e^- m^{-2} s^{-1}) with different assumed CO_2 resistances through the cell wall (r_c) and chloroplast (r_w). The model assumed Γ* and R_d were 4.31 Pa and 1.1 μmol m^{-2} s^{-1}. Parenthesis indicate the percent error in apparent C_i* and R_d relative to values assuming complete refixation of photorespired CO_2 ($r_c = 0$, $r_w = 0.3$). Slopes and y-intercepts were determined using a linear fit of 6 mesophyll CO_2 partial pressures between 2.5 and 7.5 Pa and total (See Theory).

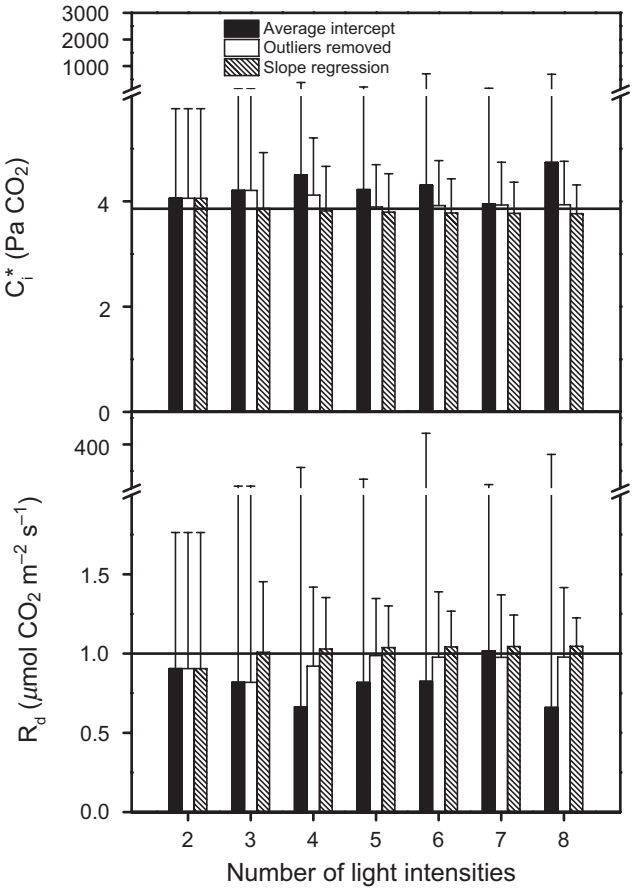

Figure 5. Simulations of C_i^* (a) and R_d (b) values determined using the common intersection method and interpreted using all averaged intersections, averaged intersections following outlier removal and using slope–intercept regression. Simulations were performed by producing an 'ideal' common intersection measurement and then introducing random variation to the initial slopes using experimental standard deviations. These simulations were performed for 2–8 light intensities with the parameterized values indicated by a solid line. Means of n = 1 000 000 ± SD simulations are shown.

Rubisco specificity does not correlate with C_i^* in meta-analysis

To determine if species-specific factors explained differences in literature C_i^* values, we compared C_i^* values with reported Rubisco specificity ($S_{c/o}$) measured at 25 °C. There was no correlation between $S_{c/o}$ and C_i^* in the six species for which both values were available in the literature despite C_i^* ranging from 2.80 to 5.31 Pa CO_2 (Fig. 7). Reported $S_{c/o}$ in these species were fairly similar and centred around 80 Pa Pa^{-1}. The two species that had higher values around 100 Pa/Pa (*Triticum aestivum* and *Limonium gibertii*) where reported from different lab groups than the other values. Γ^* derived from specificity values in plants representing adaptation to broad habitats ranged from the xerophytic *L. gibertii Sennen* (3.41 Pa) to the more mesophytic *Helleborus foetidus L.* (4.25 Pa; Supporting Information Fig. S2).

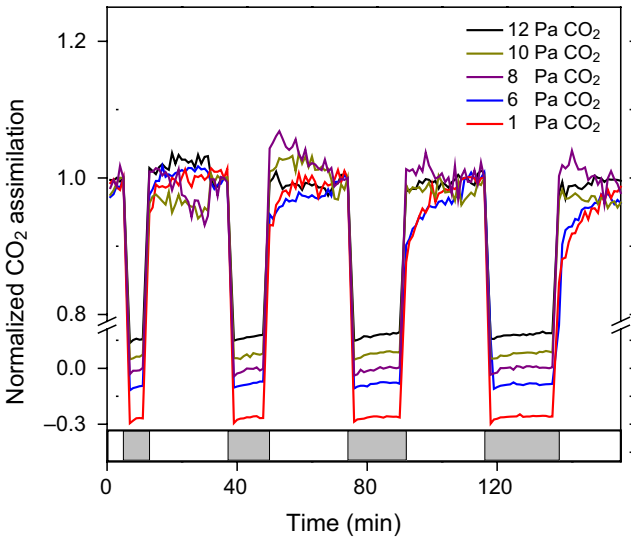

Figure 6. Impact of low CO_2 partial pressures on net CO_2 assimilation. Net CO_2 assimilation was measured in *N. tabacum* after plants had reached steady-state assimilation and conductance values at 40 Pa CO_2 and an irradiance of 390 μmol m^{-2} s^{-1}. CO_2 was then decreased to between 1 and 12 Pa CO_2 for 5 min and then returned to 40 Pa CO_2 for 25 min. This cycle was repeated with exposure to low CO_2 for 10, 15 and 20 min as indicated by the shaded portion of the lower bar. CO_2 assimilation was normalized to the value measured one minute before the drop to low CO_2 for each cycle. Means of n = 4–5 are shown.

Response of modelled *Ci** measurements to assumptions of internal CO_2 conductances

We used a modelling approach to quantify how changes in assumptions of the conductance of CO_2 from the intercellular

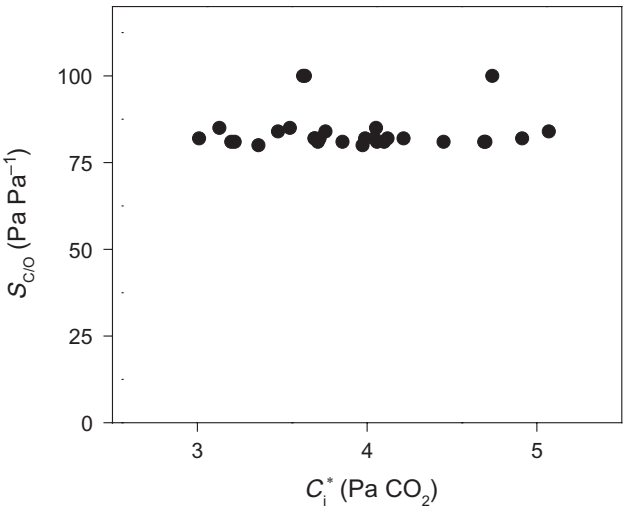

Figure 7. Rubisco specificity for reaction with CO_2 relative to O_2 ($S_{C/O}$) plotted against the intercellular CO_2 photocompensation point (C_i^*). $S_{C/O}$ values were used from (Whitney *et al.* 2011) for C_i^* values reported in Fig. 1. Shown are C_i^* values from six species with reported $S_{C/O}$.

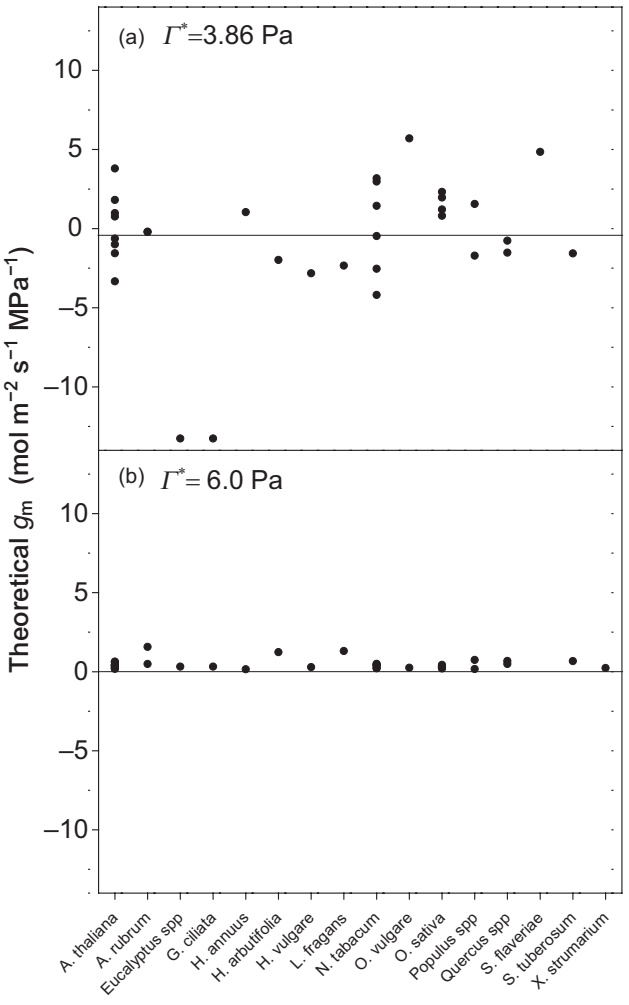

Figure 8. The theoretical mesophyll conductance (g_m) necessary to make reported C_i* values equal to a constant photocompensation point (Γ*) value of 3.86 Pa (a) and 6.0 Pa (b). The theoretical g_m was calculated for measurements of Ci* with a reported rate of day respiration (R_d) according to Eqn 2. Shown are 37 observations where R_d was recorded with three values being off the axis in panel a.

space to the chloroplast would impact the common intersections of CO_2 response curves. Since the variation in reported $S_{c/o}$ was minimal for reported C_3 species, we first determined what mesophyll conductance (g_m) would be required to explain the differences between reported C_i* assuming a constant Γ* (Fig 8, Eqns 1 & 2). We found that g_m would need to vary widely among species and individual measurements and include impossible negative values to explain the variation in C_i* assuming Γ* was equal to 3.86 Pa (8a). Since net assimilation is negative at the common intersection, Γ* would need to be greater than C_i* to result in positive g_m (Eqn 2). If Γ* were equal to 6.00 Pa, the differences between 90% of reported C_i* values could be explained with a positive g_m (Fig. 8b).

DISCUSSION

Proper selection of CO_2 range and use of slope–intercept regression can improve the accuracy and precision of C_i* determinations

Our meta-analysis indicates the need for a consistent and robust protocol for measuring and interpreting C_i* using the common intersection method. Literature-reported C_i* showed greater variation than was found in a previous comparison of Γ* values from only 12 different reports using the common intercept method (Fig. 2, Evans & Loreto 2000). This variation did not correlate with the CO_2 range used during the measurement, despite modelling which suggests that Ci* values should decrease when CO_2 measuring ranges increase (Fig. 3, Gu and Sun 2014). The insensitivity of C_i* values to measuring range suggests that literature reports of Ci* were not significantly biased by assuming linear fits or that other factors introduced more variation. This lack of CO_2 range bias could be explained if researchers selected CO_2 ranges that produced linear fits and common intersections for each species measured.

Modelling of common intersections under different ranges of CO_2 suggests that errors attributed to assumptions of linear A-C_i curves can be effectively minimized by using low measurement CO_2 partial pressure during the measurement (Fig. 3). By limiting the uppermost intercellular CO_2 partial pressure to under 10 Pa, C_i* is underestimated by only 1% and R_d by 10% (Fig. 3c). These percent underestimations are additionally insensitive to parameterized g_m or R_d values and are consistent with past predictions (Gu & Sun 2014), but quantify what the underestimation would be. This 1% underestimation would likely be within the experimental noise for gas exchange, indeed only one measurement from our meta-analysis had a standard deviation 1% of the average value and the average was 8% (Supporting Information Table S1). Given this small underestimation, it seems appropriate to use linear slopes to determine common intersections provided the uppermost intercellular CO_2 partial pressure used is under 10 Pa. However, since the impact of assuming linear relationships of A-C_i curves bias R_d much more than C_i*, care should be taken with common intersection measurements used to quantify R_d in situations where absolute values are critical (Fig. 2b,c, Harley *et al.* 1992; Gu and Sun 2014).

This modelling further suggests that while all the linear fits of A-C_i curves are not expected to intersect mathematically, their individual intersections can be very close to curvilinear intersections provided the uppermost CO_2 partial pressure is kept below ~10 Pa. The intersection of these A-C_i curves is also less sensitive to uppermost CO_2 range when the initial slopes are evenly spaced. This could explain the smaller modelled impact of linear fits that we found as compared with previous work, where two of the three initial slopes were similar (fig. 4 in Gu and Sun 2014). We therefore recommend that light intensities are selected, which give evenly spaced initial slopes.

We next examined how common intersection measurements are impacted by assumptions of intracellular

resistances to CO_2 using slope–intercept regression. Slope–intercept regression provides sensitive and quantitative analysis of the impact of multiple internal resistances to CO_2 on common intercept measurements. When r_c is large relative to r_w, there is a curvilinear relationship between the slope and y-intercept of A-C_i curves measured at sub-saturating light intensities (see Theory, Fig. 4). This curvilinear relationship was not apparent in *N. tabacum* or *G. max*, suggesting that the effective r_w was larger than r_c and that calculation of Γ^* could be made assuming simple linear resistance to CO_2 (Eqn 2).

It should be noted that this curvilinear relationship is subtle at low r_c to r_w ratios and is therefore probably not sensitive enough to directly measure small differences in r_c and r_w through fitting of 4–5 points. The slight curvilinearity is large enough, however, to significantly increase apparent C_i^* values (Table 2). Therefore, while slope–intercept regression of common intersection data may not be able to quantify small differences in the ratios of r_c to r_w, it should be able to detect larger differences. Additionally, since small differences impact C_i^*, larger apparent C_i^* values from slope-intercept regression could indicate leakage of photorespired CO_2 into the intercellular airspace. Slope–intercept regression of common intersection data thus provides a new tool to evaluate the partitioning between r_c and r_w and determine if more simple linear resistance pathways are adequate to describe CO_2 exchange.

Slope–intercept regression was more precise and accurate in determining C_i^* and R_d from A-C_i curves modelled under sub-saturating light intensities (Fig. 5). Slope–intercept regression yielded accurate values of C_i^* and R_d with less variance compared with taking the average of all intersections or taking the average of intersections following outlier removal. Slope–intercept regression also had the least variance for all measurements using more than two light intensities. It is interesting that even after 1 000 000 simulated measurements, the standard deviation of raw values with no outlier removal is expected to be very large (~300–900 for C_i^* and ~400 for R_d). Such a large standard deviation could be a result of how the simulation imposed error on generated data, but the qualitative differences between the variations in interpreting common intersection data using simple averaging versus slope–intercept regression is the same regardless of how much error is assumed in the gas exchange. Additionally, this variability in averaging all intersections may explain why despite careful technique, common intersection measurements often fail to produce common intersections, forcing either re-measurement or removal of 'outlier' data. Analysis using slope–intercept regression obviates the removal of data and results in more precise measurements of Ci* and R_d by effectively weighting the intersections of lines with similar slopes (see Theory). These simulations also demonstrate that 4–5 light intensities are optimal for C_i^* and R_d measurements and that further light intensities are not expected to greatly improve precision.

It is unclear why previous measurements of common intersections in *N. tabacum* yielded large differences in the intersection of high versus low-light A-C_i curves (Fig. 3 in Tholen *et al*. 2012). The discrepancy between our data and Tholen *et al*. (2012) may be explained by differences in leaf ages used in the measurement, since older leaves may have a decrease in the surface area of the intercellular airspace covered by chloroplasts and a larger effective ratio of r_c to r_w (Busch *et al*. 2013). Differences in the intersections of high- versus low-light A-C_i curves could also be explained through progressive deactivation of Rubisco during the measurement of high-light A-C_i curves (see below).

Appropriate selection of CO_2 measuring ranges may minimize the impact of progressive Rubisco deactivation to common intersection measurements and A-C_i curves in general. Rubisco does not appear to deactivate under moderately low CO_2 partial pressures (C_i of 14 Pa CO_2, Cen & Sage 2005), but does deactivate near the CO_2 compensation point (Caemmerer & Edmondson 1986). Our findings indicated that the impact of CO_2 partial pressure on Rubisco activation state could be time dependent (Fig. 6). There was no apparent deactivation of Rubisco evident from the net CO_2 assimilation rate at 40 Pa CO_2 following 5 min exposure to between 1 and 12 Pa CO_2. Rubisco appeared to deactivate slightly following ten minutes of exposure to 1 and 6 Pa CO_2 but net CO_2 exchange returned to starting values after less than 5 min upon return to 40 Pa CO_2. After 15 and 20 min of exposure to 1 and 6 Pa CO_2, Rubisco appeared to take much longer to reactivate. Exposure to 8 Pa CO_2 and above had no effect on Rubisco activation state even after 20 min (Fig. 6). These findings indicate that common intersection measurements should not remain below ~8 Pa CO_2 for longer than ~10 min to maintain Rubisco activation state. To balance the need to measure under low CO_2 to minimize the impact of using linear fits with the danger of Rubisco deactivation, we suggest starting each light intensity at 40 Pa CO_2 and then measuring at 5–6 CO_2 partial pressures between 3 and 10 Pa to determine the initial slope and y-intercept. We also recommend returning to 40 Pa CO_2 before changing the light intensity to determine if Rubisco deactivation occurred at the lower CO_2 Pa. These recommendations are based on measurements in *N. tabacum* and could vary based on interspecies differences in Rubisco activation.

The temperature response of literature C_i^* values is different than that commonly used to parameterize leaf models of photosynthesis

The differences in the temperature response of C_i^* between literature values and that of *N. tabacum* could be due to *N. tabacum* having an unusually high temperature response as compared with other species (Fig. 2b). The increased temperature response of C_i^* could be due to differences in the temperature response of g_m, since *N. tabacum* has among the largest temperature response and absolute values of g_m compared to eight other species (von Caemmerer & Evans 2014). Larger g_m values result in increased C_i^* assuming constant $S_{c/o}$ and R_d (Eqns 1 & 2). Alternatively, the temperature response of C_i^* in *N. tabacum* could be due to either an unusually decreased temperature sensitivity of $S_{c/o}$ or an decreased sensitivity of R_d relative to other species. It is interesting that the literature temperature response of C_i^* closely resembles the response of *A. thaliana*, suggesting that species other than tobacco might more broadly represent the

temperature response of C_i* for modelling (Fig. 2b). Clearly, more work is needed confirming the temperature response of C_i*, Γ* and g_m across ecologically and agronomically important species to determine the most appropriate temperature functions to use in leaf scale or earth system models.

Alternatively, since the *N. tabacum* temperature response was originally determined and since confirmed by growing plants in a controlled environment with day temperatures between 23 and 25 °C and then temporarily moving plants to higher or lower temperatures for measurement of C_i* (Bernacchi *et al*. 2001; Walker & Cousins 2013; Walker *et al*. 2013). This approach would not account for species-specific differences in the temperature response of C_i*, the absolute values of C_i* or an acclimation of C_i* that could occur during longer-term exposure to elevated temperature.

Differences in the temperature response or acclimation of $S_{c/o}$ could also explain some of the variation in C_i* found in the literature among species (Eqns 1 and 2). Such acclimation would result in plants grown at higher temperatures having decreased C_i* values when measured near their growth temperature. Indeed, measurement temperature was within 2 °C of growth temperature for 70% of C_i* values with reported growth temperature (Supporting information Table S1). There is some evidence that $S_{c/o}$ acclimates to growth temperature by differential expression of Rubisco small subunit genes, which would result in decreased C_i* at high temperatures (Cavanagh & Kubien 2014). This differential expression could explain the observation that the temperature response of *in vitro* Γ* in spinach leaves is decreased in plants grown under elevated temperature (Yamori *et al*. 2006). Such an acclimation response of $S_{c/o}$ is consistent with the differences seen between literature values primarily measured near growth temperatures and those reported in (Bernacchi *et al*. 2001; Fig. 2a).

Differences in $S_{c/o}$ among species could also explain differences in C_i* values, although there was no significant interaction between species and C_i* values normalized to 25 °C. This lack of interaction could be explained by improper temperature response normalization functions or noisy measurement technique. Alternatively, this variation could be due to differences among species due to adaptation of $S_{c/o}$ (Sage 2002; Galmés *et al*. 2005). When $S_{c/o}$ measured in a diversely adapted group of species were converted to Γ*, there was a less variation than we observed in the literature (Fig. 2, Supporting Information Fig. S1). It is also possible that methodological differences between labs could explain the lack of correlation between $S_{c/o}$ and C_i*, but we would still expect to see some correlation since most of the reported $S_{c/o}$ and measurements came from the same group. These observations suggest that typical variation in $S_{c/o}$ is not large enough to significantly impact measurements of C_i* and do not explain the variation in reported values.

To understand if differences in internal conductance to CO_2 could explain the variation in C_i*, we modelled the impact of different linear conductance pathways to measurements of C_i*. The range of mesophyll conductances needed to make literature C_i* values equal a common Γ* value of 3.86 Pa are larger than what has been reported in the literature and include impossible negative conductances (Fig. 6a; Warren 2008; Niinemets *et al*. 2009). To result in only positive conductances, Γ* needs to be greater than the assumed C_i* assuming a single mesophyll conductance (Eqn 2). Γ* would need to be 6.0 Pa to be greater than 90% of the literature reported C_i* measurements, which is almost twice as large as what is predicted from a wide range of $S_{c/o}$ values in higher C3 plants (Fig. 8b, Supporting Information Fig. S1). These findings suggest that differences in g_m do not alone explain the variation in observed C_i* assuming a single diffusive path of CO_2. These analysis on previous data confirm that much of the variation reported in C_i* is not due to physiological factors (differences in $S_{c/o}$ or g_m), but to methodological issues with the measurement. Such potential for methodological error highlights the importance of adapting a robust and consistent protocol (e.g. slope–intercept analysis) for measuring C_i*.

It should be noted that it is possible for Γ* to be less than C_i* assuming multiple diffusive resistances if r_c is much larger than r_w (Eqns 4 & 5; Tholen *et al*. 2012). Assuming a simple linear diffusion path, physical modelling of CO_2 resistance based on leaf anatomy suggests r_w could account for 50% or more of total resistance and the contribution of r_c ranges significantly (Evans *et al*. 2009). Assuming RuBP-limited photosynthesis and, a J value of 75 μmol electrons $e^- m^{-2} s^{-1}$, and an R_d of 2, r_c would need to be ~3 times greater than r_w for Γ* to be less than C_i* (Eqn 5). We found no evidence of such a large ratio of r_c to r_w in our slope–intercept measurements for *N. tabacum* and *G. max* but it is possible this ratio is variable in other species. Additionally, to explain the differences in reported C_i* values, the ratio of r_w relative to r_c would need to be highly variable within species since both positive and negative g_m values were required to explain a common Γ* value in both *A. thaliana* and *N. tabacum* (Fig. 6a).

CONCLUSIONS

Slope–intercept regression provides a robust and precise analysis tool for determining C_i* and R_d from CO_2 gas exchange. Slope–intercept analysis can help determine if multiple resistances within the cell to CO_2 should be considered and what their impact would be. This analysis offers significant improvement over traditional intersection averaging and is less sensitive to experimental noise. We found that biases introduced by using linear fits to interpret curvilinear data could be minimized by measuring with CO_2 ranges under 10 Pa and that predicted variation is optimal when 4–5 light intensities are used. Our meta-analysis shows significant variation in reported C_i* values and evidence that commonly used temperature response functions of C_i*, and by extension Γ*, needs to be re-examined for species diversity and possible acclimation.

ACKNOWLEDGMENTS

Jessica Ayers for technical assistance during common intersection measurements and Susanne von Caemmerer for

helpful thoughts on the modelling and discussion points. Thomas Sharkey also provided insight for technical considerations for the common intersection method and helped spawn this study in the first place. We would also like to thank two anonymous reviewers for thoughtful comments that greatly broadened the scope of our analysis and discussion. This research was supported via subcontract by the Bill and Melinda Gates Foundation (OPP1060461) titled 'RIPE-Realizing Increased Photosynthetic Efficiency for Sustainable Increases in Crop Yield'.

REFERENCES

Balaguer L., Afif D., Dizengremel P. & Dreyer E. (1996) Specificity factor of ribulose bisphosphate carboxylase/oxygenase of *Quercus robur*. *Plant Physiology and Biochemistry* **34,** 879–883.

Bernacchi C.J., Pimentel C. & Long S.P. (2003) In vivo temperature response functions of parameters required to model RuBP-limited photosynthesis. *Plant, Cell & Environment* **26,** 1419–1430.

Bernacchi C.J., Portis A.R., Nakano H., von Caemmerer S. & Long S.P. (2002) Temperature response of mesophyll conductance. Implications for the determination of Rubisco enzyme kinetics and for limitations to photosynthesis *in vivo*. *Plant Physiology* **130,** 1992–1998.

Bernacchi C.J., Singsaas E.L., Pimentel C., Portis A.R. & Long S.P. (2001) Improved temperature response functions for models of Rubisco-limited photosynthesis. *Plant, Cell & Environment* **24,** 253–259.

Berry J., Collatz G., Guy R. & Fogel M. (1994) The compensation point: can a physiological concept be applied to global cycles of carbon and oxygen. *Regulation of Atmospheric CO_2 and O_2 by Photosynthetic Carbon Metabolism*, pp. 234–248. Oxford University Press, Oxford.

Brooks A. & Farquhar G.D. (1985) Effect of temperature on the CO_2/O_2 specificity of ribulose-1, 5-bisphosphate carboxylase/oxygenase and the rate of respiration in the light. *Planta* **165,** 397–406.

Bunce J.A. (1998) The temperature dependence of the stimulation of photosynthesis by elevated carbon dioxide in wheat and barley. *Journal of Experimental Botany* **49,** 1555–1561.

Busch F.A., Sage T.L., Cousins A.B. & Sage R.F. (2013) C_3 plants enhance rates of photosynthesis by reassimilating photorespired and respired CO_2. *Plant, Cell & Environment* **36,** 200–212.

Caemmerer S. & Edmondson D. (1986) Relationship between steady-state gas exchange, in vivo ribulose bisphosphate carboxylase activity and some carbon reduction cycle intermediates in Raphanus sativus. *Australian Journal of Plant Physiology* **13,** 669–688.

Cano F.J., Sánchez-Gómez D., Gascó A., Rodríguez-Calcerrada J., Gil L., Warren C.R. & Aranda I. (2011) Light acclimation at the end of the growing season in two broadleaved oak species. *Photosynthetica* **49,** 581–592.

Cavanagh A.P. & Kubien D. (2014) Can phenotypic plasticity in Rubisco performance contribute to photosynthetic acclimation? *Photosynthesis Research* **119,** 203–214.

Cen Y.-P. & Sage R.F. (2005) The regulation of Rubisco activity in response to variation in temperature and atmospheric CO_2 partial pressure in sweet potato. *Plant Physiology* **139,** 979–990.

Cousins A.B., Walker B.J., Pracharoenwattana I., Smith S.M. & Badger M.R. (2011) Peroxisomal hydroxypyruvate reductase is not essential for photorespiration in arabidopsis but its absence causes an increase in the stoichiometry of photorespiratory CO_2 release. *Photosynthesis Research* **108,** 91–100.

Cronquist A. (1981) *An Integrated System of Classification of Flowering Plants*, Columbia University Press.

Douthe C., Dreyer E., Brendel O. & Warren C.R. (2012) Is mesophyll conductance to CO_2 in leaves of three Eucalyptus species sensitive to short-term changes of irradiance under ambient as well as low O_2? *Functional Plant Biology* **39,** 435–448.

Drewry D.T., Kumar P., Long S., Bernacchi C., Liang X.Z. & Sivapalan M. (2010) Ecohydrological responses of dense canopies to environmental variability: 1. Interplay between vertical structure and photosynthetic pathway. *Journal of Geophysical Research* **115,** G04022.

Duda R.O. & Hart P.E. (1972) Use of the Hough transformation to detect lines and curves in pictures. *Communications of the ACM* **15,** 11–15.

Evans J. & Loreto F. (2000) Acquisition and diffusion of CO_2 in higher plant leaves. In *Photosynthesis: Physiology and Metabolism* (eds R.C. Leegood, T.D. Sharkey & S. von Caemmerer), pp. 321–351. Kluwer Academic Publishers, Dordrecht, The Netherlands.

Evans J.R., Kaldenhoff R., Genty B. & Terashima I. (2009) Resistances along the CO_2 diffusion pathway inside leaves. *Journal of Experimental Botany* **60,** 2235–2248.

Flexas J., Ortuño M.F., Ribas-Carbo M., Diaz-Espejo A., Flórez-Sarasa I.D. & Medrano H. (2007) Mesophyll conductance to CO_2 in *Arabidopsis thaliana*. *The New Phytologist* **175,** 501–511.

Galmés J., Flexas J., Keys A.J., Cifre J., Mitchell R.A.C., Madgwick P.J., . . . Parry M.A.J. (2005) Rubisco specificity factor tends to be larger in plant species from drier habitats and in species with persistent leaves. *Plant, Cell & Environment* **28,** 571–579.

Galmés J., Medrano H.L. & Flexas J. (2006) Acclimation of Rubisco specificity factor to drought in tobacco: discrepancies between *in vitro* and *in vivo* estimations. *Journal of Experimental Botany* **57,** 3659–3667.

Gilbert M.E., Pou A., Zwieniecki M.A. & Holbrook N.M. (2012) On measuring the response of mesophyll conductance to carbon dioxide with the variable J method. *Journal of Experimental Botany* **63,** 413–425.

Giuliani R., Koteyeva N., Voznesenskaya E., Evans M.A., Cousins A.B. & Edwards G.E. (2013) Coordination of leaf photosynthesis, transpiration, and structural traits in rice and wild relatives (Genus *Oryza*). *Plant Physiology* **162,** 1632–1651.

Gu L. & Sun Y. (2014) Artefactual responses of mesophyll conductance to CO_2 and irradiance estimated with the variable *J* and online isotope discrimination methods. *Plant, Cell & Environment* **37,** 1231–1249.

Guo S., Schinner K., Sattelmacher B. & Hansen U.-P. (2005) Different apparent CO_2 compensation points in nitrate-and ammonium-grown *Phaseolus vulgaris* and the relationship to non-photorespiratory CO_2 evolution. *Physiologia Plantarum* **123,** 288–301.

Harley P., Loreto F., Di Marco G. & Sharkey T. (1992) Theoretical considerations when estimating the mesophyll conductance to CO2 flux by analysis of the response of photosynthesis to CO_2. *Plant Physiology* **98,** 1429–1436.

Häusler R.E., Kleines M., Uhrig H., Hirsch H.-J. & Smets H. (1999) Overexpression of phosphoenolpyruvate carboxylase from *Corynebacterium glutamicum* lowers the CO_2 compensation point (Γ^*) and enhances dark and light respiration in transgenic potato. *Journal of Experimental Botany* **50,** 1231–1242.

Igamberdiev A., Mikkelsen T., Ambus P., Bauwe H., Lea P. & Gardeström P. (2004) Photorespiration contributes to stomatal regulation and carbon isotope fractionation: a study with barley, potato and Arabidopsis plants deficient in glycine decarboxylase. *Photosynthesis Research* **81,** 139–152.

Jacob J. & Lawlor D.W. (1993) Extreme phosphate deficiency decreases the *in vivo* CO_2/O_2 specificity factor of ribulose 1,5-bisphosphate carboxylase-oxygenase in intact leaves of sunflower. *Journal of Experimental Botany* **44,** 1635–1641.

Kebeish R., Niessen M., Thiruveedhi K., Bari R., Hirsch H.-J., Rosenkranz R., . . . Peterhansel C. (2007) Chloroplastic photorespiratory bypass increases photosynthesis and biomass production in *Arabidopsis thaliana*. *Nature Biotechnology* **25,** 593–599.

Kirschbaum M. & Farquhar G. (1984) Temperature dependence of whole-leaf photosynthesis in *Eucalyptus pauciflora* Sieb. Ex Spreng. *Functional Plant Biology* **11,** 519–538.

Laisk A. (1977) Kinetics of photosynthesis and photorespiration in C_3 plants. Nauka, Moscow (in Russian).

LI-COR Biosciences (2010) Modification of LI-6400/LI-6400XT to control at low [CO_2]. LI-COR application note Application note 7.

Li Y., Gao Y., Xu X., Shen Q. & Guo S. (2009) Light-saturated photosynthetic rate in high-nitrogen rice (*Oryza sativa* L.) leaves is related to chloroplastic CO_2 concentration. *Journal of Experimental Botany* **60,** 2351–2360.

Niinemets U., Wright I.J. & Evans J.R. (2009) Leaf mesophyll diffusion conductance in 35 Australian sclerophylls covering a broad range of foliage structural and physiological variation. *Journal of Experimental Botany* **60,** 2433–2449.

Peisker M. & Apel H. (2001) Inhibition by light of CO_2 evolution from dark respiration: comparison of two gas exchange methods. *Photosynthesis Research* **70,** 291–298.

Pons T.L. & Westbeek M.H.M. (2004) Analysis of differences in photosynthetic nitrogen-use efficiency between four contrasting species. *Physiologia Plantarum* **122,** 68–78.

R Core Team (2013) *R: A Language and Environment for Statistical Computing*, R Foundation for Statistical Computing, Vienna, Austria. (URL: http://www.R-project.org/).

Rogers A., Medlyn B.E. & Dukes J.S. (2014) Improving representation of photosynthesis in Earth System Models. *The New Phytologist* **204,** 12–14.

Sage R.F. (2002) Variation in the k_{cat} of Rubisco in C_3 and C_4 plants and some implications for photosynthetic performance at high and low temperature. *Journal of Experimental Botany* **53,** 609–620.

Sage R.F. & Kubien D.S. (2007) The temperature response of C_3 and C_4 photosynthesis. *Plant, Cell & Environment* **30,** 1086–1106.

Sage T.L., Busch F.A., Johnson D.C., Friesen P.C., Stinson C.R., Stata M., . . . Sage R.F. (2013) Initial events during the evolution of C4 photosynthesis in C3 species of *Flaveria*. *Plant Physiology* **163,** 1266–1276.

Schneidereit J., Häusler R.E., Fiene G., Kaiser W.M. & Weber A.P.M. (2006) Antisense repression reveals a crucial role of the plastidic 2-oxoglutarate/malate translocator DiT1 at the interface between carbon and nitrogen metabolism. *The Plant Journal* **45,** 206–224.

Tholen D., Ethier G., Genty B., Pepin S. & Zhu X.-G. (2012) Variable mesophyll conductance revisited: theoretical background and experimental implications. *Plant, Cell & Environment* **35,** 2087–2103.

Tholen D. & Zhu X.-G. (2011) The mechanistic basis of internal conductance: a theoretical analysis of mesophyll cell photosynthesis and CO_2 diffusion. *Plant Physiology* **156,** 90–105.

Tomaz T., Bagard M., Pracharoenwattana I., Linden P., Lee C.P., Carroll A.J., . . . Millar A.H. (2010) Mitochondrial malate dehydrogenase lowers leaf respiration and alters photorespiration and plant growth in Arabidopsis. *Plant Physiology* **154,** 1143–1157.

USDA (2015) The PLANTS Database. http://plants.usda.gov.

Villar R., Held A.A. & Merino J. (1994) Comparison of methods to estimate dark respiration in the light in leaves of two woody species. *Plant Physiology* **105,** 167–172.

von Caemmerer S. (2000) *Biochemical Models of Leaf Photosynthesis*, Vol. **2,** CSIRO, Collingwood.

von Caemmerer S. (2013) Steady-state models of photosynthesis. *Plant, Cell & Environment* **36,** 1617–1630.

von Caemmerer S., Evans J., Hudson G. & Andrews T. (1994) The kinetics of ribulose-1, 5-bisphosphate carboxylase/oxygenase in vivo inferred from measurements of photosynthesis in leaves of transgenic tobacco. *Planta* **195,** 88–97.

von Caemmerer S. & Evans J.R. (2014) Temperature responses of mesophyll conductance differ greatly between species. *Plant, Cell & Environment* **38,** 629–637.

von Caemmerer S. & Farquhar G.D. (1981) Some relationships between the biochemistry of photosynthesis and the gas exchange of leaves. *Planta* **153,** 376–387.

Walker B., Ariza L.S., Kaines S., Badger M.R. & Cousins A.B. (2013) Temperature response of in vivo Rubisco kinetics and mesophyll conductance in *Arabidopsis thaliana*: comparisons to *Nicotiana tabacum*. *Plant, Cell & Environment* **36,** 2108–2119.

Walker B. & Cousins A. (2013) Influence of temperature on measurements of the CO_2 compensation point: differences between the Laisk and O_2-exchange methods. *Journal of Experimental Botany* **64,** 1893–1905.

Walker B.J., Strand D.D., Kramer D.M. & Cousins A.B. (2014) The response of cyclic electron flow around photosystem I to changes in photorespiration and nitrate assimilation. *Plant Physiology* **165,** 453–462.

Warren C. & Dreyer E. (2006) Temperature response of photosynthesis and internal conductance to CO_2: results from two independent approaches. *Journal of Experimental Botany* **57,** 3057–3067.

Warren C.R. (2008) Stand aside stomata, another actor deserves centre stage: the forgotten role of the internal conductance to CO_2 transfer. *Journal of Experimental Botany* **59,** 1475–1487.

Weise S., Carr D., Bourke A., Hanson D.T., Swarthout D. & Sharkey T. (2015) The arc mutants of Arabidopsis with fewer large chloroplasts have a lower mesophyll conductance. *Photosynthesis Research* 1–10.

Weston D.J., Bauerle W.L., Swire-Clark G.A., Moore B. & Baird W.V. (2007) Characterization of Rubisco activase from thermally contrasting genotypes of *Acer rubrum* (Aceraceae). *American Journal of Botany* **94,** 926–934.

Whitney S.M., Houtz R.L. & Alonso H. (2011) Advancing our understanding and capacity to engineer nature's CO_2-sequestering enzyme, Rubisco. *Plant Physiology* **155,** 27–35.

Yamori W., Suzuki K., Noguchi K., Nakai M. & Terashima I. (2006) Effects of Rubisco kinetics and Rubisco activation state on the temperature dependence of the photosynthetic rate in spinach leaves from contrasting growth temperatures. *Plant, Cell and Environment* **29,** 1659–1670.

Zhu X.-G., Long S.P. & Ort D.R. (2008) What is the maximum efficiency with which photosynthesis can convert solar energy into biomass? *Current Opinion in Biotechnology* **19,** 153–159.